This is an open access article published under an ACS AuthorChoice License, which permits copying and redistribution of the article or any adaptations for non-commercial purposes.

ACS OMEGA

Article

http://pubs.acs.org/journal/acsodf

Piezoresistive Response of Quasi-One-Dimensional ZnO Nanowires Using an in Situ Electromechanical Device

Sören Kaps,[*,†] Sanjit Bhowmick,[*,‡] Jorit Gröttrup,[†] Viktor Hrkac,[†] Douglas Stauffer,[‡] Hua Guo,[§,∥] Oden L. Warren,[‡] Jost Adam,[⊥] Lorenz Kienle,[†] Andrew M. Minor,[§,∥] Rainer Adelung,[†] and Yogendra Kumar Mishra[*,†]

[†]Institute for Materials Science, Kiel University, Kaiserstraße 2, D-24143 Kiel, Germany

[‡]Bruker Nano Surfaces, Minneapolis, Minnesota 55344, United States

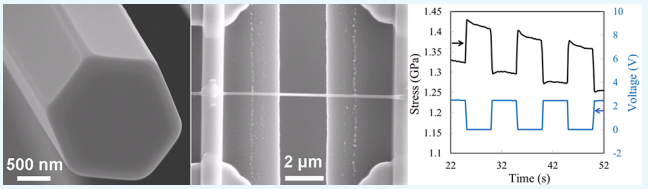
[§]Department of Materials Science and Engineering, University of California Berkeley, Berkeley, California 94720, United States

[∥]National Center for Electron Microscopy, Molecular Foundry, Lawrence Berkeley National Laboratory, Berkeley, California 94720, United States

[⊥]Mads Clausen Institute, NanoSYD, University of Southern Denmark, Alsion 2, DK-6400 Sønderborg, Denmark

Supporting Information

ABSTRACT: Quasi-one-dimensional structures from metal oxides have shown remarkable potentials with regard to their applicability in advanced technologies ranging from ultra-responsive nanoelectronic devices to advanced healthcare tools. Particularly due to the piezoresistive effects, zinc oxide (ZnO)-based nanowires showed outstanding performance in a large number of applications, including energy harvesting, flexible electronics, smart sensors, etc. In the present work, we demonstrate the versatile crystal engineering of ZnO nano- and microwires (up to centimeter length scales) by a simple flame transport process. To investigate the piezoresistive properties, particular ZnO nanowires were integrated on an electrical push-to-pull device, which enables the application of tensile strain and measurement of in situ electrical properties. The results from ZnO nanowires revealed a periodic variation in stress with respect to the applied periodic potential, which has been discussed in terms of defect relaxations.



1. INTRODUCTION

Quasi-one-dimensional (Q1D) structures, such as nanorods, nanowires, nanotubes, and nanobelts, etc. of inorganic materials have shown remarkable potential with regard to their utilization in several applications ranging from ultraresponsive nanoelectronic devices to advanced healthcare diagnostic systems.[1−7] Nanowires consisting of metal oxide semiconductors have drawn particular research interest because of their high surface to volume ratios, unique shapes and surface morphologies, application-relevant bandgaps, particular crystal structures, bendability, etc.[8−11] These Q1D nanowire structures have already shown significant potential in the context of energy storage in the form of photovoltaics, solar cells, electrochemical cells, and supercapacitors.[12−15] Both, the size and the crystal structure play an important role in enabling the advanced applications of Q1D nanostructures. Recently, a new class of application for nanowires, so-called self-powered devices, has emerged, in which the nanowire is utilized as a power generator for driving an electronic device under the influence of some external stimuli, such as stress, temperature, or UV light.[16−20] In this context, zinc oxide (ZnO) has garnered significant research interest because of its wide and direct UV-sensitive bandgap (∼3.37 eV) and large exciton binding energy (∼60 meV).[21,22] On the one hand, the hexagonal-wurtzite-type structure facilitates easy growth of various types of Q1D structures from ZnO, and on the other hand, the absence of an inversion center enables piezoelectric property in these Q1D nanowires.[21,22] These piezoelectric and semiconductor properties have resulted in research focuses for applications in piezoresistive or piezotronics, piezophototronics, and energy-harvesting devices.[23−31] Owing to their biocompatible and luminescent (blue and green) features, the ZnO nanorods and nanowires exhibit significant potentials for utilizations in advanced sensing devices and in biomedical applications.[32−35] Thus, equipped with interesting functionalities, Q1D ZnO nanostructures are potential key candidates for the next generation of advanced technologies.

Despite their quite high technological relevancy, these Q1D nano- and micro-structures strongly suffer from device integration issues. To measure the properties, the nanowire structures need to be properly connected with the test instrumentation, representing a complicated task. Owing to the dimensions, placing nanowires at the desired location and aligning them to form appropriate electrical contacts are the challenging steps in nanoelectronic device fabrications. This sometimes requires a multistep fabrication process.[3,4,36−39] To

Received: January 12, 2017
Accepted: June 13, 2017
Published: June 28, 2017

 © 2017 American Chemical Society

DOI: 10.1021/acsomega.7b00041
ACS Omega 2017, 2, 2985−2993

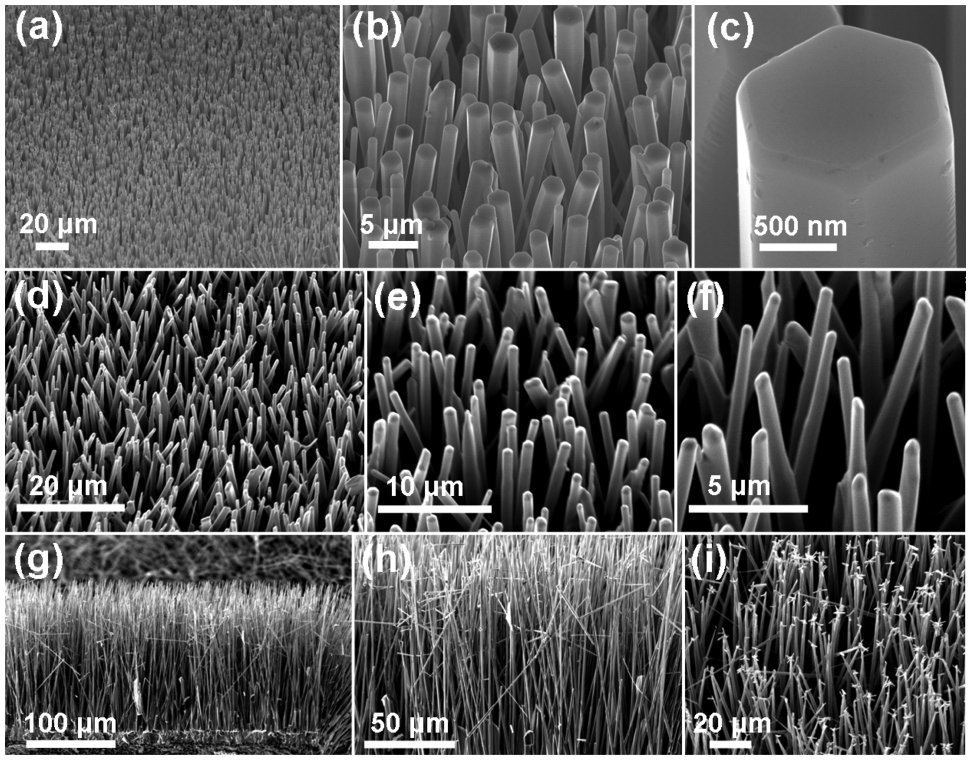


Figure 1. SEM morphologies at increasing magnifications (left to right, low to high) of different Q1D ZnO nano- and microwires synthesized by the FTS approach on Si substrates. (a–c) Homogeneous array of hexagonally faceted Q1D ZnO nanowires. (d–f) Array of Q1D ZnO nano- and microwires with smooth surfaces. (g–i) Side-view SEM images of a dense array of relatively longer (>200 μm length) Q1D ZnO nano- and microwires grown on a Si substrate. These Q1D ZnO microwires are very well interconnected with the base and are almost homogeneous in diameter (bottom to top) with a sharp needle-like tip at their ends. The growth of smaller flower-like ZnO nanostructures on their tips is mainly due to secondary growth (the denser array of wires favors growth on the tips).

overcome these barriers, several unconventional strategies[40−42] have been introduced, but simpler nanodevice fabrication is still highly desired. In general, the Q1D nanostructure-based electronic devices are fabricated in two ways: (i) synthesis of nanowires (physical, chemical, or biological routes), followed by their integration between the electrical contacts on the patterned microchips; and (ii) fabrication of Q1D nanostructures directly on the microchips. For the versatile utilization of Q1D structures, the synthesis of dimensionally compact nanowires by simple processes is one of the first and foremost requirement. Free-standing Q1D nano- and micro-structures with diameters in the submicron region and lengths up to several hundred micrometers seem to be very suitable candidates in this context as they can be very easily utilized in various ways. However, controlled growth of such large nano- and microwires that possess adequate structural integrity requires sophisticated growth methods.

In this respect, the recently introduced flame transport synthesis (FTS) approach has shown unique potential in terms of a simple growth process and versatile structuring (from 1D to three-dimensional interconnected networks).[43,44] Because 1D structures are the main focus of this study, controlled growth of ZnO Q1D nano- and micro-structures with size scales spanning from nanometers to centimeters by the FTS approach in a simple, rapid, and single-step process is presented here. An important variable to the understanding of piezoresistive properties is the type of strain applied to an individual nanorod. Prior studies have generally utilized the bending of a substrate or piezoforce microscope to apply the strain in the nanowires.[45] Owing to the unavailability of appropriate devices that can grip and apply tensile strain in individual nanowires, the experimental studies for characterizing the electrical properties under tensile stress are lacking. In general, a typical piezoelectrical device consists of a semiconductor nanostructure with a noncentrosymmetric crystal structure, such as ZnO, GaN, etc., with two metallic electrodes connected at both ends. Therefore, the change in electronic transport properties in such devices combines the piezoresistive effect in the nanowire and a possibility of a piezotronic effect from the two contacts at the end.[45−47] In this article, we demonstrate a novel in situ characterization strategy for direct measurement of electrical properties of the nanowires and present an effect of piezoresistive response of the Q1D ZnO nanowires under tensile strain. To the best of our knowledge, this is the first study revealing the detailed quantitative electromechanical characterization of an ultralarge Q1D ZnO single crystalline nanowire under tensile strain.

2. RESULTS AND DISCUSSION

The appropriate length scales together with the desirable morphologies of Q1D structures are important aspects playing major roles with regard to their structure−property relations as well as corresponding technological applications. Therefore, the growth of large varieties of Q1D ZnO nano- and microstructures would be highly desirable, and this can be easily achieved by the developed FTS approach.[43] By varying the experimental parameters, Q1D ZnO wires with length scales ranging from a few hundred nanometers to almost a centimeter have been successfully grown, as demonstrated by the scanning electron microscopy (SEM) images in Figures 1 and 2. Just for

DOI: 10.1021/acsomega.7b00041
ACS Omega 2017, 2, 2985−2993

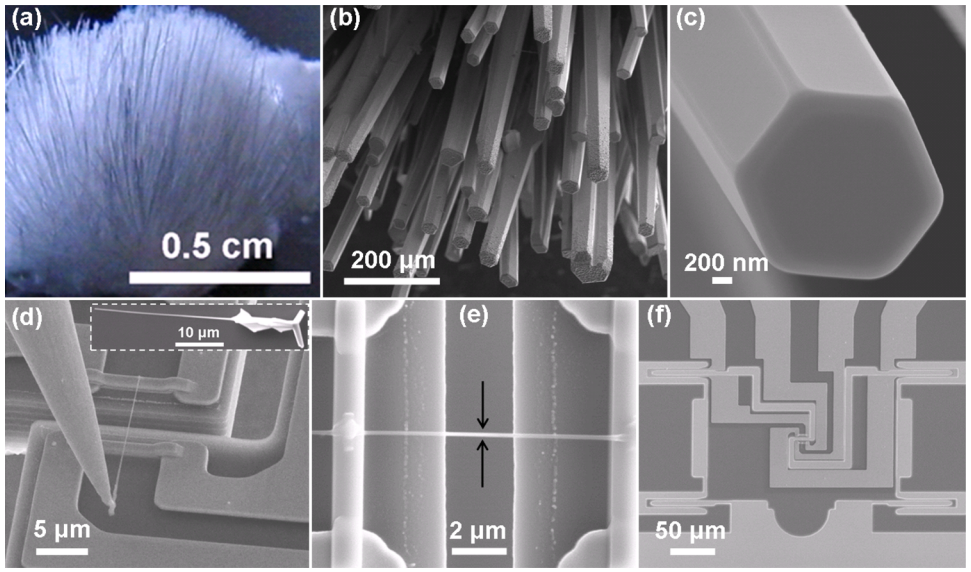


Figure 2. Q1D ZnO nano- and microwires from one particular synthesis batch were selected for electrical push-to-pull (E-PTP) studies. (a) Digital photograph of a typical edge of a Si wafer where a bunch of Q1D ZnO wires are grown after the FTS process. (b, c) Typical SEM images from the synthesized Q1D ZnO nano- and microwires at low and high magnifications, respectively. ZnO nanowires were carefully harvested from the bunch (a) and mounted on the E-PTP device. Representative SEM images (d–f) of the mounted (using a nanomanipulator) Q1D ZnO nanowire on the E-PTP device.

demonstration, the only selected morphological variants of three different types of Q1D ZnO nanowires grown by the FTS approach are presented here; however, growth of many other 1D structural variants from ZnO is possible. The array of hexagonal Q1D ZnO nanowires (on a Si substrate) is shown by SEM images at increasing magnifications (left to right) in Figure 1a–c. The highest-magnification SEM image, corresponding to a single nanorod in Figure 1c, clearly shows the hexagonally faceted morphology. The growth of a dense array of regular ZnO nanowires by the FTS process is demonstrated by the SEM images in Figure 1d–f at increasing magnifications (left to right). These nanowires are almost uniform in dimension (length and diameter) and cylindrical in shape (circular cross section). It is important to emphasize here that mechanical integration of Q1D ZnO nano- and microwires with Si has always been an issue, and different strategies (particular crystal facets, adhesion promoters, surface roughness, etc.) have been utilized. The FTS approach does not exhibit such requirements, and well-integrated Q1D ZnO structures on Si surfaces can be easily grown.[35] For better visualization, side-view SEM images (low and high magnification) corresponding to the growth of a forest of 1D ZnO nanowires on a Si substrate by the FTS process are shown in Figure 1g,i, respectively. It can be observed that these long ZnO nano- and microwires are very well connected to the Si substrate and have a highly dense array. The top-view SEM image (Figure 1i) reveals that some of the Q1D ZnO nanowires in the "forest" exhibit small branches on their tips.

The crystallographic structure and experimental arrangements play a very important role for morphological evolutions of Q1D ZnO structures in the FTS approach. Owing to the hexagonal-wurtzite structure, ZnO has three fast growth directions, [0001], [10$\bar{1}$0], and [2$\bar{1}\bar{1}$0], with growth rates (r) ranked in the order of $r_{[0001]} > r_{[01\bar{1}0]} > r_{[000\bar{1}]}$.[48,49] The (0001) facet is the least stable surface that facilitates easy growth of Q1D ZnO structures, and their morphology (diameter, length, surface quality, etc.) mainly depends upon the chosen synthesis technique and experimental parameters.[48,49] In the FTS approach here, growth of Q1D ZnO nano- and microwires occurs via a solid–vapor–solid process using an in-house cylindrically arranged ceramic in a furnace at high temperature (~900 °C) in the presence of O_2, CO, and CO_2 gases, which provide local control over the growth conditions.[43,48] The synthesis temperature (~900 °C) in the FTS approach leads to the sublimation of the solid Zn microparticles (present in the precursor—Zn + PVB + ethanol mixture) into Zn atomic vapor, and the decomposition of a sacrificial polymer [poly(vinyl butyral) (PVB)] facilitates the availability of local control gases.[48] ZnO nucleation begins at the exposed surfaces of the mounted Si substrates, followed by subsequent 1D growth. It has been observed that Q1D wires in nano and submicron scales primarily grow on the main surface (facing toward the precursor material)[43] of the Si substrates; however, longer Q1D wires (from the submillimeter to centimeter scale) grow on the cleaved surfaces (perpendicular to the precursor mixture) of the substrates. The growth of longer Q1D ZnO nanowires at the perpendicular edges is most likely attributed to: (i) a faster nucleation process (due to the presence of defects during cleavage of the Si wafer); and (ii) the greater availability of the Zn and O atomic species. Further experiments using a bigger crucible have also supported this assumption because the growth of subcentimeter-long nano- and micro-wires on their periphery (inner surface) has also been observed. It is important to mention here that utilization of a silicon substrate is not at all a mandatory requirement; in fact, ZnO nanowires can grow on the surface of large ZnO nano- and micro-structures because of the surface defects.[15,43,50] In the FTS approach, it is a self-controlled growth process in which the pregrown ZnO structures serve as possible nucleation centers (due to the existence of a large number of surface defects) for the growth of 1D ZnO nanowires, for example, nanowire forests and branched structures, etc.[15,43,50,51] Therefore, for such applications, in which free-standing nanowires are required, the simple crucible strategy in the

DOI: 10.1021/acsomega.7b00041
ACS Omega 2017, 2, 2985–2993

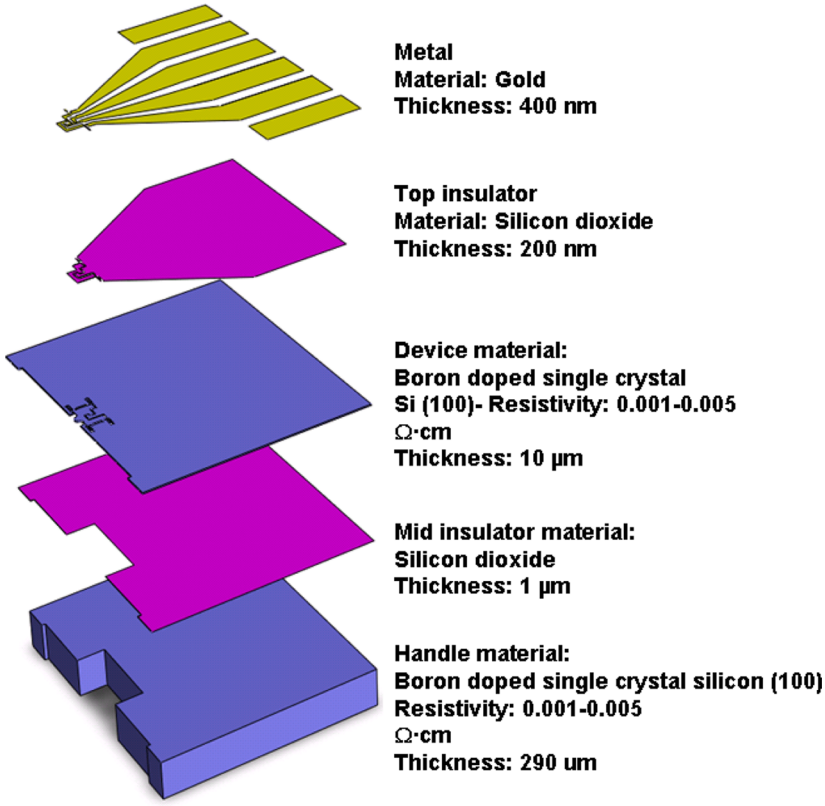


Figure 3. Schematic of an E-PTP device shows the dimensions and materials in different layers.[54]

FTS approach (no need of any substrate) suits best because a large number of Q1D ZnO nano- and microwires are directly grown on a pile, and they can be easily harvested for desired utilizations (e.g., Figure 2a). Thus, by selecting appropriate experimental conditions (precursor amount, temperature, time, substrate location, etc.) in the FTS approach, various types of Q1D ZnO nano- and microwires can be easily grown for desired utilizations.

As mentioned previously, the dimensions (diameter, length, etc.) of the Q1D ZnO nanostructures play a crucial role with regard to their integration in the form of nanoelectronic devices[45] and in investigating their responses, especially in electromechanical studies in which very strong and reliable interconnections are desired. The larger the Q1D ZnO nanowires, the simpler and more free they are from the aforementioned utilization complexities. Inspired with these advantages, we were motivated to grow the ultralong Q1D ZnO nanowires using the FTS approach. After varying the parameters (mixture of precursor materials, internal arrangement), the growth of ultralong Q1D ZnO wires (almost up to a centimeter) was successfully realized, as presented in Figure 2a–c. A lot of such ZnO nano- and microwires nicely grow from the big ZnO base (digital photograph in Figure 2a), which can easily be harvested and used for any desired applications. The SEM investigations on a typical ultralong ZnO nanowire revealed that they exhibit hexagonal facets, mainly due to the *c* axis growth nature of ZnO (Figure 2b,c). The most important aspects are that even these ZnO nano- and microwires are very long in size, they are perfectly single crystalline in nature,[52,53] and they exhibit most of the desired nanoscale features, which make them appropriate structures for building reliable nanoelectronic devices.

Some selected Q1D ZnO nanowires with sufficiently large lengths (>20 μm) have been utilized for in situ electromechanical studies using an electrical push-to-pull (E-PTP) device (Bruker Nano Surfaces). The E-PTP device was designed in such a way that it enables tensile testing of individual nanowires with a high degree of precession while simultaneously measuring the electrical properties.[54] The sample preparation for the E-PTP device is demonstrated in the SEM images (Figure 2d–f). To collect individual samples, the nanowires were removed from the growth substrate and placed on a silicon substrate (inset in Figure 2d). Individual nanowires were then picked up by a nanowire of a manipulator and placed on the E-PTP device (Figure 2d). A Pt-based gas injection system (GIS) was used for mechanically securing the Q1D ZnO nanowires to the E-PTP device, while also creating the electrical contacts with the electrical leads of the system. To reduce Pt spreading over the nanowire, the Pt pads were first deposited, followed by the Q1D ZnO nanowire placement (shown by the high-magnification SEM image in Figure 2e). Figure 2f shows an overview of the E-PTP device with the integrated electrical leads. When the movable part of the E-PTP is pushed with an indentation system, the sample mounted across the 2.5 μm gap experiences the applied tensile strain.

Figure 3 shows the fabrication details of the E-PTP device, which consists of five layers.[54] The top layer (gold ∼400 nm thick) is used to make the electrical connections to the sample and to wire bond the leads to a circuit board. The next layer (∼200 nm SiO_2) electrically isolates the gold leads and the silicon device layer. The deep trenches on the device layer and the top oxide layer isolate each electrode. The mechanical components, such as springs and the movable electrode, are designed on the 10 μm thick device layer. This device layer has been designed to be passively mobile when pushed by the tip

DOI: 10.1021/acsomega.7b00041
ACS Omega 2017, 2, 2985−2993

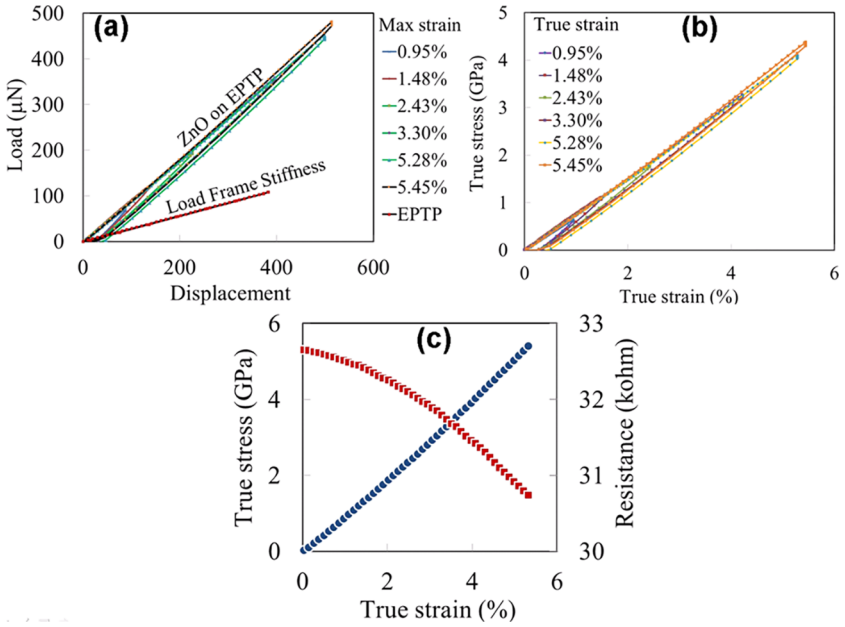


Figure 4. (a, b) Load–displacement and stress–strain curves of Q1D ZnO nanowire tensile experiments at different strains. (c) Stress–strain and resistance–strain curves obtained during tensile experiments of a Q1D ZnO nanowire. A constant voltage of 0.5 V was applied during the test and the current was measured.

on the semicircular part. This device layer has orders of magnitude higher stiffness in the lateral and out-of-plane directions to restrict all motion to the uniaxial tensile direction. This stiffness, characteristic for tensile testing, is achieved by carefully designing the springs using a finite element analysis. The 1 μm silicon oxide layer insulates the device and the handle layer. A 350 μm thick bottom layer is used to provide the necessary strength to protect the device and specimen during handling. It is very important to mention that the E-PTP device just facilitates simple fabrication of the nanowire-based electronic device. However, for electromechanical sensing, an additional transducer would be required, which is a SEM PicoIndenter PI 85 in the present work.

The mechanical responses of the ZnO nanowires measured using the E-PTP device are shown in Figure 4a,b. The load–displacement curves (under zero electrical bias) obtained from the SEM PicoIndenter are given in Figure 4a. It is important to note that the Q1D ZnO nanowire exhibits predominantly elastic behavior, as expected, up to a displacement of ∼550 nm, followed by a catastrophic fracture. True stress and true strain were determined using the force–displacement data and plotted in Figure 4b. The actual force to the Q1D ZnO nanowire was calculated by subtracting the E-PTP frame stiffness from the experimentally measured load, measured here as 320 N/m. The elastic modulus from the stress–strain curves was calculated to be 82 ± 1.8 GPa. The reported values of the elastic modulus of ZnO nanowires or nanobelts are widely scattered between 50 and 140 GPa.[55] In this study, the nanowire fractured at ∼5.9% strain, which is significantly higher than the fracture strain of bulk ZnO (<1%). Hoffmann et al.[56] and Chen and Zhu[57] have also reported the fracture strain of ZnO nanowires to be 4–8 and 4–7%, respectively. As expected in the brittle fracture of a ceramic material, no necking or evidence of ductility was observed during the failure. The high fracture strain evidenced in the present nanowire samples may be due to their crystalline nature in contrast to a bulk sample.[52,58] Because the fracture occurs by crack nucleation from a defect, the probability of failure has been significantly reduced simply due to the lower sampled volume. The electromechanical behavior of the Q1D ZnO nanowires was then explored in a separate set of experiments where a fixed bias voltage of 0.5 V was applied across the outer two contacts on the nanowire during a tensile test. This enabled the measurement of the current as a function of the strain. Figure 4c shows the stress–strain and resistance–strain curves from such a test. The resistance was calculated assuming ohmic behavior. A 2 kΩ decrease in the measured resistance was observed under a corresponding strain of up to 5.5%.

The detailed piezoresistive responses from two individual Q1D ZnO nanowires are presented in Figure 5. The inset in Figure 5a shows a schematic of a typical load function that was used to conduct such experiments. Voltage sweeps of ±0.3 V were applied during the holding segments at different applied strain values. The characteristic $I-V$ curves shown in Figure 5a are linear and symmetric indicating ohmic behavior. Previous studies have reported that such ohmic contacts of ZnO nanowires with metal electrodes are possible, and the characteristic $I-V$ curves were determined by the surface condition, crystallinity, chemical reaction, and the work functions.[59] The slopes of the $I-V$ curves and sample dimensions were used to calculate the resistivity of the nanowire material (sample 1), which is plotted in Figure 5b. To understand the variation in the resistivity under strain, E-PTP measurements on a second Q1D ZnO nanowire (sample 2) were repeated under identical conditions, and the corresponding values are plotted in Figure 5b. Both samples exhibit similar electromechanical change, and the decrease in the resistivity values were calculated to be 14.2 and 13.9% with a maximum applied strain of ∼4.25 and 4.34%, respectively (Figure 5b). In most of the previous studies, the gauge factor is mainly determined by bending a substrate and calculating the corresponding strain[60] or bending a nanowire,[23] which includes significant theoretical approximations. The piezoresistance is

DOI: 10.1021/acsomega.7b00041
ACS Omega 2017, 2, 2985–2993

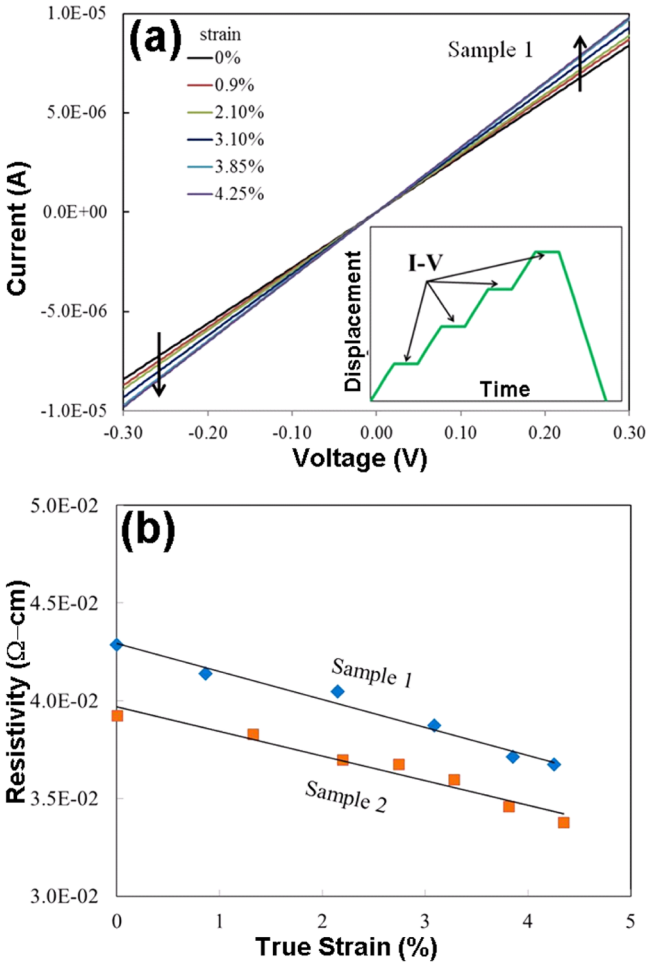


Figure 5. (a) $I-V$ characteristic curves obtained from a 1D ZnO nanowire 1 showing the change in slope with applied strain. (b) Resistivity vs strain curve showing a decrease in the electrical resistivity of 14.2% in sample 1 and 13.9% in sample 2.

defined as the change of the resistance under applied strain and is described by a gauge factor (G) in eq 1

$$G = \frac{\Delta R}{R} \Big/ \frac{\Delta l}{l} \tag{1}$$

Precise measurements of the gauge factor offer a much more realistic way to understand the actual response of a piezoresistive device. The control of the applied strain using the SEM PicoIndenter equipped with the E-PTP device, as shown in this study, provides a very precise measurement of the gauge factors and hence a better accuracy, in contrast to the conventional bending methods used previously in the literature.[60] For both Q1D ZnO nanowires, as shown in Figure 5b, the average gauge factor values are −3.26 and −3.32. The small variation in the obtained values (<2%) shows the excellent reproducibility of the electromechanical measurements on Q1D ZnO nanowires using the E-PTP device.

To elucidate the piezoresistive behavior, a constant strain of 4.25% was adjusted to the Q1D ZnO nanowire (sample 1) while a rectangular potential of 0−2.4 V was applied. Under fixed strain, the internal stress developed in the Q1D ZnO nanowire caused by the variation in the applied voltage was measured as a change of the closed loop force required to maintain the constant strain. This variation in the internal stress with respect to the applied voltage is shown in Figure 6. Although the stress change ($\Delta\sigma$) due to the voltage variation is

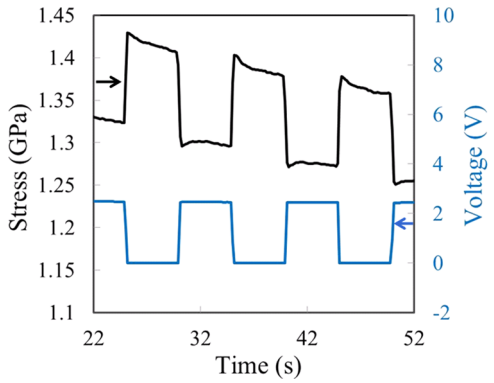


Figure 6. Variation in stress in the Q1D nanowire under periodic potentials.

found to be similar in the segments, a stress relaxation can certainly be observed during the hold period. This observed stress relaxation could be attributed to several factors, such as migration of point defects, surface reconstructions, a variation in the carrier electron density at the surfaces, or an interplay between the inner core and surface contributions of the stressed Q1D ZnO nano- and microwires.[61−66] Different types of defects in ZnO nanowires exhibit a variety of diffusivities under stress, resulting in significant inelastic strain behavior and thus an instantaneous stress relaxation,[61,67] which is most likely the case in the present observations. The results in this study demonstrate that the applied tensile strain can considerably enhance the electrical conductivity of the Q1D ZnO nanowires. It has been reported that a bent ZnO nanowire displays the opposite behavior, that is, the conductivity decreases with an increase in strain.[29] However, in the case of bending, the layers at the outer and inner arc surfaces of a bent Q1D ZnO nanowire produce positively and negatively charged surfaces, respectively (Supporting Information, Figure S1).[68,69] As described by Yang et al., the charges are considered as immobile ionic charges, creating an electric field across the width of the ZnO nanowires.[29] This local electrical field across the width of a ZnO nanowire traps electrons, causing the decrease in the total electron concentration and hence mobility along the length direction. In contrast, a ZnO nanowire strained in pure tension enhances the electron concentration and mobility.[68]

Defects play an important role in different properties, and an accurate defect handling/modeling is still a debatable issue.[21,66,67] Although the utilized Q1D ZnO nanowires are single crystalline in nature, they exhibit lots of intrinsic defects, including unavoidable surface defects, which definitely impact the observed electromechanical piezoresistive response in the present work. For a better understanding, the finite element method (FEM) simulations were performed using standard ZnO physical parameters under identical experimental conditions as in the E-PTP. The preliminary FEM (COMSOL Multiphysics) modeling observations nicely support the experimental results in terms of periodic variations (current/stress) under the application of periodic potentials and vice versa; however, the stress values differ by certain factors. We currently address this issue to the above-mentioned various kinds of defects, which would need to be carefully considered

DOI: 10.1021/acsomega.7b00041
ACS Omega 2017, 2, 2985−2993

during FEM simulations. For more detailed mechanistic insights, a comparative study with both the experimental and FEM simulation studies needs to be performed on a set of Q1D ZnO nanowire dimensions, under different experimental conditions. This is planned as a detailed future study. Such studies would be of interest for a large number of material engineering communities, and they will also facilitate potential applications involving strain engineering. Depending upon the conditions, the amount and the nature of the strain, the bandgap of the Q1D nanostructured materials can be tuned, implicating technological importance for various advanced electronic devices, including piezoresistive/piezotronic transistors and other self-powered electronic appliances. In the conventional field effect transistor, an electrical potential is applied between the device's source and drain to create an electrical field, which controls the current flow. In the piezotronic transistors, current flow can be controlled by changing the conductivity of the nanostructure material by just bending or stretching. This study shows that nanowire stretching can change the conductivity and thus can be used as a "gate potential" in related electronic devices, in which the amount of gate potential is directly related to the amount of applied tensile strain.

3. CONCLUSIONS

In summary, we have demonstrated here the successful growth of ultralong Q1D free-standing ZnO nano- and microwires by a single-step flame transport process. Because this process is flexible with respect to the dimensions of the synthesized structures, these nano- and microwires can be easily integrated into reliable devices designed for a wide variety of intended applications. Here, we have made an attempt to understand the effect of the piezoresistance behavior of the Q1D ZnO nanowires using an E-PTP device in conjunction with an in situ SEM indentation system. These Q1D ZnO nanowires were electrically mounted on E-PTP devices, and their detailed electromechanical responses were measured in situ. The electromechanical results revealed that the electrical conductivity of the Q1D ZnO nanowires increased significantly with an applied tensile strain. The observed periodic variations in stress with respect to the applied periodic potentials on the prestressed Q1D ZnO nanowire confirmed the piezoresistive effect from the Q1D ZnO nanowires. Defect relaxations play a very important role on the piezoresistive response of ZnO, which has been discussed in detail here. The characteristics of these Q1D ZnO nano- and microwires under applied strain could be useful for various electronic, energy-harvesting, stress-sensing, self-powered devices, and other advanced technological applications.

4. EXPERIMENTAL DETAILS

4.1. Synthesis of Q1D ZnO Nanowires. Q1D ZnO nano- and microwires were grown by the FTS approach using Zn microparticles (diameter <10 μm, 99.5%, Goodfellow, U.K.), PVB sacrificial polymer powder (Kuraray GmbH, Europe), and ethanol in a single-step process inside a simple muffle-type furnace.[35,43,48,70] A homogeneous mixture [Zn:(PVB:ethanol)::1:2(1:2)] in the form of a slurry is used as the precursor material. An in-house ceramic cylindrical setup (inner diameter 55 mm, height around 55 mm) was inserted inside the furnace to achieve the local control on Zn vapor (upward flow only) inside the furnace. The precursor material is mounted at the bottom of the cylinder, and the growth of arrays of Q1D ZnO nano- and microwires takes place on the Si substrates mounted on the top (with the help of a ceramic cover). For the nanowire array growth, the temperature is generally varied from 850 to 950 °C for a time span of 30 min to 4 h. Lower temperature/growth durations are preferable for thinner nanowire arrays; however, higher temperatures and durations yield thicker and longer Q1D nano- and microwire arrays. For exceptionally long (centimeter scale) Q1D ZnO wires, a different top cover arrangement is utilized (thin ceramic strips are mounted along the diameter of the cylinder), and Si strips are placed on the top of the ceramic strip (the ceramic strip role is to support the Si substrates). The whole cylindrical arrangement is inserted in the furnace, which is then rapidly heated to 900 °C and maintained for a couple of hours (1−2 h, depending upon the requirements). After the process, the growth of ZnO nanowires occurs on the edges of the Si strips as well as on the top. The FTS growth process only requires a simple muffle-type oven, and the synthesis has been carried out in normal air atmosphere. The recent experiment suggests that the growth of Q1D ZnO nano- and micro-structures is possible directly by the use of a large cylindrical ceramic crucible (without cylindrical arrangement) filled with a Zn/PVB mixture in the ratio of 1:2. However, the observations suggest that the cylinder approach offers much more control in comparison to the crucible-only approach. After growth, a few Q1D ZnO nanowires with a diameter 0.3−0.4 μm and length 20 μm were carefully harvested and utilized for the desired electromechanical experiments.

4.2. Characterizations. The morphology of the grown ZnO nano- and microwires was characterized by a Zeiss Ultraplus (5 kV, 15 μA) SEM machine at the Kiel University, and afterward, they were transported to Hysitron, Inc. for in situ E-PTP studies. The ZnO nanowire was mounted on the E-PTP device with the help of a nanomanipulator inside a dual-beam SEM-FIB machine. The E-PTP device was used only for mounting the nanowire sample and to pass the current across it. A commercially available transducer was used with the system (SEM PicoIndenter PI 85; Bruker Nano Surfaces, Minneapolis, MN), which controls actuation and sensing. The Pt-based GIS was used to weld Q1D ZnO nanowires, and the contacts were connected with electrical leads outside. The in situ electromechanical studies were performed by the PI 85 nanomechanical instrument (Bruker Nano Surfaces Division) inside a field emission SEM. A direct current source meter was used to apply and measure the current and voltage. To obtain electrical properties as a function of strain, the nanowires were stretched to different lengths and voltage sweeps were applied at fixed strains. To understand the piezoresistive behavior, periodic voltages were applied across the length of the Q1D nanowires and the corresponding stresses were measured.

■ ASSOCIATED CONTENT

Supporting Information

The Supporting Information is available free of charge on the ACS Publications website at DOI: 10.1021/acsomega.7b00041.

Distribution of charge carriers and variation in bandgap in ZnO nanowires under mechanical deformations (Figures S1) (PDF)

DOI: 10.1021/acsomega.7b00041
ACS Omega 2017, 2, 2985−2993

AUTHOR INFORMATION

Corresponding Authors

*E-mail: ska@tf.uni-kiel.de (S.K.).
*E-mail: Sanjit.Bhowmick@bruker.com (S.B.).
*E-mail: ykm@tf.uni-kiel.de (Y.K.M.).

ORCID

Jost Adam: 0000-0001-7177-3252
Yogendra Kumar Mishra: 0000-0002-8786-9379

Notes

The authors declare no competing financial interest.

ACKNOWLEDGMENTS

Authors from Kiel University acknowledge the support from German Research Foundation (DFG) under the scheme SFB 1261, TP {(A05, RA) & (A06, LK)}. Work at the Molecular Foundry was supported by the Office of Science, Office of Basic Energy Sciences, of the U.S. Department of Energy under Contract No. DE-AC02-05CH11231. Authors from Bruker Nano Surfaces would like to thank Dr. Yunje Oh for designing and developing E-PTP devices and providing a schematic of the device.

REFERENCES

(1) Friedman, R. S.; McAlpine, M. C.; Ricketts, D. S.; Ham, D.; Lieber, C. M. Nanotechnology: High-speed Integrated Nanowire Circuits. *Nature* **2005**, *434*, 1085.

(2) Goldberger, J.; Sirbuly, D. J.; Law, M.; Yang, P. ZnO Nanowire Transistors. *J. Phys. Chem. B* **2005**, *109*, 9−14.

(3) Thelander, C.; Agarwal, P.; Brongersma, S.; Eymery, J.; Feiner, L. F.; Forchel, A.; Scheffler, M.; Riess, W.; Ohlsson, B. J.; Gösele, U.; et al. Nanowire-based One-dimensional Electronics. *Mater. Today* **2006**, *9*, 28−35.

(4) Patolsky, F.; Timko, B. P.; Zheng, G.; Lieber, C. M. Nanowire-based Nanoelectronic Devices in the Life Sciences. *MRS Bull.* **2007**, *32*, 142−149.

(5) Yan, R.; Gargas, D.; Yang, P. Nanowire Photonics. *Nat. Photonics* **2009**, *3*, 569−576.

(6) Chen, K.-I.; Li, B.-R.; Chen, Y.-T. Silicon Nanowire Field-effect Transistor-based Biosensors for Biomedical Diagnosis and Cellular Recording Investigation. *Nano Today* **2011**, *6*, 131−154.

(7) Paulowicz, I.; Hrkac, V.; Kaps, S.; Cretu, V.; Lupan, O.; Braniste, T.; Duppel, V.; Tiginyanu, I.; Kienle, L.; Adelung, R.; et al. Three-Dimensional SnO_2 Nanowire Networks for Multifunctional Applications: From High-Temperature Stretchable Ceramics to Ultra-responsive Sensors. *Adv. Electron. Mater.* **2015**, *1*, No. 1500081.

(8) Tian, B.; Liu, X.; Yang, H.; Xie, S.; Yu, C.; Tu, B.; Zhao, D. General Synthesis of Ordered Crystallized Metal Oxide Nanoarrays Replicated by Microwave-Digested Mesoporous Silica. *Adv. Mater.* **2003**, *15*, 1370−1374.

(9) Kolmakov, A.; Moskovits, M. Chemical Sensing and Catalysis by One-dimensional Metal-oxide Nanostructures. *Annu. Rev. Mater. Res.* **2004**, *34*, 151−180.

(10) Thangala, J.; Vaddiraju, S.; Bogale, R.; Thurman, R.; Powers, T.; Deb, B.; Sunkara, M. K. Large-Scale, Hot-Filament-Assisted Synthesis of Tungsten Oxide and Related Transition Metal Oxide Nanowires. *Small* **2007**, *3*, 890−896.

(11) Comini, E.; Sberveglieri, G. Metal Oxide Nanowires as Chemical Sensors. *Mater. Today* **2010**, *13*, 36−44.

(12) Hochbaum, A. I.; Yang, P. Semiconductor Nanowires for Energy Conversion. *Chem. Rev.* **2010**, *110*, 527−546.

(13) Tian, B.; Kempa, T. J.; Lieber, C. M. Single Nanowire Photovoltaics. *Chem. Soc. Rev.* **2009**, *38*, 16−24.

(14) Bae, J.; Song, M. K.; Park, Y. J.; Kim, J. M.; Liu, M.; Wang, Z. L. Fiber Supercapacitors Made of Nanowire-Fiber Hybrid Structures for Wearable/Flexible Energy Storage. *Angew. Chem., Int. Ed.* **2011**, *50*, 1683−1687.

(15) Cheng, C.; Fan, H. J. Branched Nanowires: Synthesis and Energy Applications. *Nano Today* **2012**, *7*, 327−343.

(16) Soci, C.; Zhang, A.; Xiang, B.; Dayeh, S. A.; Aplin, D.; Park, J.; Bao, X.; Lo, Y.-H.; Wang, D. ZnO Nanowire UV Photodetectors with High Internal Gain. *Nano Lett.* **2007**, *7*, 1003−1009.

(17) Wang, Z. L. Towards Self-Powered Nanosystems: From Nanogenerators to Nanopiezotronics. *Adv. Funct. Mater.* **2008**, *18*, 3553−3567.

(18) Xu, S.; Qin, Y.; Xu, C.; Wei, Y.; Yang, R.; Wang, Z. L. Self-powered Nanowire Devices. *Nat. Nanotechnol.* **2010**, *5*, 366−373.

(19) Cha, S. N.; Seo, J. S.; Kim, S. M.; Kim, H. J.; Park, Y. J.; Kim, S. W.; Kim, J. M. Sound-Driven Piezoelectric Nanowire-Based Nanogenerators. *Adv. Mater.* **2010**, *22*, 4726−4730.

(20) Wu, W.; Bai, S.; Yuan, M.; Qin, Y.; Wang, Z. L.; Jing, T. Lead Zirconate Titanate Nanowire Textile Nanogenerator for Wearable Energy-harvesting and Self-powered Devices. *ACS Nano* **2012**, *6*, 6231−6235.

(21) Wang, Z. L. ZnO Nanowire and Nanobelt Platform for Nanotechnology. *Mater. Sci. Eng., R* **2009**, *64*, 33−71.

(22) Özgür, Ü.; Alivov, Y. I.; Liu, C.; Teke, A.; Reshchikov, M. A.; Doğan, S.; Avrutin, V.; Cho, S.-J.; Morkoç, H. A Comprehensive Review of ZnO Materials and Devices. *J. Appl. Phys.* **2005**, *98*, No. 041301.

(23) Wang, X.; Zhou, J.; Song, J.; Liu, J.; Xu, N.; Wang, Z. L. Piezoelectric Field Effect Transistor and Nanoforce Sensor based on a Single ZnO Nanowire. *Nano Lett.* **2006**, *6*, 2768−2772.

(24) Wang, Z. L.; Song, J. Piezoelectric nanogenerators based on zinc oxide nanowire arrays. *Science* **2006**, *312*, 242−246.

(25) Wang, Z. L. The New Field of Nanopiezotronics. *Mater. Today* **2007**, *10*, 20−28.

(26) Zhou, J.; Gu, Y.; Fei, P.; Mai, W.; Gao, Y.; Yang, R.; Bao, G.; Wang, Z. L. Flexible Piezotronic Strain Sensor. *Nano Lett.* **2008**, *8*, 3035−3040.

(27) Wang, Z. L. Progress in Piezotronics and Piezo-phototronics. *Adv. Mater.* **2012**, *24*, 4632−4646.

(28) Zhang, Y.; Yan, X.; Yang, Y.; Huang, Y.; Liao, Q.; Qi, J. Scanning Probe Study on the Piezotronic Effect in ZnO Nanomaterials and Nanodevices. *Adv. Mater.* **2012**, *24*, 4647−4655.

(29) Yang, S.; Wang, L.; Tian, X.; Xu, Z.; Wang, W.; Bai, X.; Wang, E. The Piezotronic effect of Zinc Oxide Nanowires Studied by *in-situ* TEM. *Adv. Mater.* **2012**, *24*, 4676−4682.

(30) Zhang, R.; Andersson, H.; Olsen, M.; Hummelgård, M.; Edvardsson, S.; Nilsson, H.-E.; Olin, H. Piezoelectric Gated ZnO Nanowire Diode Studied by *In-situ* TEM Probing. *Nano Energy* **2014**, *3*, 10−15.

(31) Wu, W.; Wang, L.; Li, Y.; Zhang, F.; Lin, L.; Niu, S.; Chenet, D.; Zhang, X.; Hao, Y.; Heinz, T. F.; et al. Piezoelectricity of Single-atomic-layer MoS_2 for Energy Conversion and Piezotronics. *Nature* **2014**, *514*, 470−474.

(32) Chu, S.; Wang, G.; Zhou, W.; Lin, Y.; Chernyak, L.; Zhao, J.; Kong, J.; Li, L.; Ren, J.; Liu, J. Electrically Pumped Waveguide Lasing from ZnO Nanowires. *Nat. Nanotechnol.* **2011**, *6*, 506−510.

(33) Li, Z.; Yang, R.; Yu, M.; Bai, F.; Li, C.; Wang, Z. L. Cellular Level Biocompatibility and Biosafety of ZnO Nanowires. *J. Phys. Chem. C* **2008**, *112*, 20114−20117.

(34) Antoine, T. E.; Hadigal, S. R.; Yakoub, A. M.; Mishra, Y. K.; Bhattacharya, P.; Haddad, C.; Valyi-Nagy, T.; Adelung, R.; Prabhakar, B. S.; Shukla, D. Intravaginal Zinc Oxide Tetrapod Nanoparticles as Novel Immunoprotective Agents against Genital Herpes. *J. Immunol.* **2016**, *196*, 4566−4575.

(35) Reimer, T.; Paulowicz, I.; Röder, R.; Kaps, S.; Lupan, O.; Chemnitz, S.; Benecke, W.; Ronning, C.; Adelung, R.; Mishra, Y. K. Single Step Integration of ZnO Nano-and Microneedles in Si Trenches by Novel Flame Transport Approach: Whispering Gallery Modes and Photocatalytic Properties. *ACS Appl. Mater. Interfaces* **2014**, *6*, 7806−7815.

(36) Huang, Y.; Duan, X.; Lieber, C. M. Nanowires for Integrated Multicolor Nanophotonics. *Small* **2005**, *1*, 142−147.

DOI: 10.1021/acsomega.7b00041
ACS Omega 2017, 2, 2985−2993

(37) Menke, E. J.; Thompson, M. A.; Xiang, C.; Yang, L. C.; Penner, R. M. Lithographically Patterned Nanowire Electrodeposition. *Nat. Mater.* **2006**, *5*, 914−919.
(38) Goldberger, J.; Hochbaum, A. I.; Fan, R.; Yang, P. Silicon Vertically Integrated Nanowire Field Effect Transistors. *Nano Lett.* **2006**, *6*, 973−977.
(39) Bernal, R. A.; Filleter, T.; Connell, J. G.; Sohn, K.; Huang, J.; Lauhon, L. J.; Espinosa, H. D. In Situ Electron Microscopy Four-Point Electromechanical Characterization of Freestanding Metallic and Semiconducting Nanowires. *Small* **2014**, *10*, 725−733.
(40) Xia, Y.; Rogers, J. A.; Paul, K. E.; Whitesides, G. M. Unconventional Methods for Fabricating and Patterning Nanostructures. *Chem. Rev.* **1999**, *99*, 1823−1848.
(41) Adelung, R.; Aktas, O. C.; Franc, J.; Biswas, A.; Kunz, R.; Elbahri, M.; Kanzow, J.; Schurmann, U.; Faupel, F. Strain-controlled Growth of Nanowires within Thin-film Cracks. *Nat. Mater.* **2004**, *3*, 375−379.
(42) Rao, K.; Gupta, R.; Kulkarni, G. U. Fabrication of Large Area, High-Performance, Transparent Conducting Electrodes Using a Spontaneously Formed Crackle Network as Template. *Adv. Mater. Interfaces* **2014**, *1*, No. 1400090.
(43) Mishra, Y. K.; Kaps, S.; Schuchardt, A.; Paulowicz, I.; Jin, X.; Gedamu, D.; Freitag, S.; Claus, M.; Wille, S.; Kovalev, A.; et al. Fabrication of Macroscopically Flexible and Highly Porous 3D Semiconductor Networks from Interpenetrating Nanostructures by a Simple Flame Transport Approach. *Part. Part. Syst. Charact.* **2013**, *30*, 775−783.
(44) Hölken, I.; Neubüser, G.; Postica, V.; Bumke, L.; Lupan, O.; Baum, M.; Mishra, Y. K.; Kienle, L.; Adelung, R. Sacrificial Template Synthesis and Properties of 3-D Hollow-silicon Nano- and Microstructures. *ACS Appl. Mater. Interfaces* **2016**, *8*, 20491−20498.
(45) Gröttrup, J.; Kaps, S.; Carstensen, J.; Smazna, D.; Mishra, Y. K.; Piorra, A.; Kirchhof, C.; Quandt, E.; Adelung, R. Piezotronic-based Magnetoelectric Sensor: Fabrication and Response. *Phys. Status Solidi A* **2016**, *213*, 2208−2215.
(46) Peng, M.; Liu, Y.; Yu, A.; Zhang, Y.; Liu, C.; Liu, J.; Wu, W.; Zhang, K.; Shi, X.; Kou, J.; et al. Flexible Self-Powered GaN Ultraviolet Photoswitch with Piezo-Phototronic Effect Enhanced On/Off Ratio. *ACS Nano* **2016**, *10*, 1572−1579.
(47) Zhang, Y.; Liu, C.; Liu, J.; Xiong, J.; Liu, J.; Zhang, K.; Liu, Y.; Peng, M.; Yu, A.; Zhang, A.; et al. Lattice Strain Induced Remarkable Enhancement in Piezoelectric Performance of ZnO-Based Flexible Nanogenerators. *ACS Appl. Mater. Interfaces* **2016**, *8*, 1381−1387.
(48) Mishra, Y. K.; Modi, G.; Cretu, V.; Postica, V.; Lupan, O.; Reimer, T.; Paulowicz, I.; Hrkac, V.; Benecke, W.; Kienle, L.; Adelung, R. Direct Growth of Freestanding ZnO Tetrapod Networks for Multifunctional Applications in Photocatalysis, UV Photodetection and Gas Sensing. *ACS Appl. Mater. Interfaces* **2015**, *7*, 14303−14316.
(49) Zhan, J.; Dong, H.; Sun, S.; Ren, X.; Liu, J.; Chen, Z.; Lienau, C.; Zhang, L. Surface-Energy-Driven Growth of ZnO Hexagonal Microtube Optical Resonators. *Adv. Opt. Mater.* **2016**, *4*, 126−134.
(50) Kargar, A.; Sun, K.; Jing, Y.; Choi, C.; Jeong, H.; Jung, G. Y.; Jin, S.; Wang, D. 3D Branched nanowire photoelectrochemical electrodes for efficient solar water splitting. *ACS Nano* **2013**, *7*, 9407−9415.
(51) Ko, S. H.; Lee, D.; Kang, H. W.; Nam, K. H.; Yeo, J. Y.; Hong, S. J.; Grigoropoulos, C. P.; Sung, H. J. Nanoforest of Hydrothermally Grown Hierarchical ZnO Nanowires for a High Efficiency Dye-sensitized Solar Cell. *Nano Lett.* **2011**, *11*, 666−671.
(52) Hrkac, S.; Abes, M.; Koops, C.; Krywka, C.; Müller, M.; Kaps, S.; Adelung, R.; McCord, J.; Lage, E.; Quandt, E.; et al. Local Magnetization and Strain in Single Magnetoelectric Microrod Composites. *Appl. Phys. Lett.* **2013**, *103*, No. 123111.
(53) Hrkac, S.; Koops, C.; Abes, M.; Krywka, C.; Mueller, M.; Burghammer, M.; Sztucki, M.; Dane, T.; Kaps, S.; Mishra, Y. K. et al. Tunable Strain in Magnetoelectric ZnO Micro Rod Composite Interfaces. *ACS Appl. Mater, Interfaces*, submitted for publication, 2017.
(54) Oh, Y.; Cyrankowski, E.; Shan, Z.; Asif, S. A. S. U.S. Patent US8434370 B2, 2013.
(55) Wen, B.; Sader, J. E.; Boland, J. J. Mechanical Properties of ZnO Nanowires. *Phys. Rev. Lett.* **2008**, *101*, No. 175502.
(56) Hoffmann, S.; Östlund, F.; Michler, J.; Fan, H.; Zacharias, M.; Christiansen, S.; Ballif, C. Fracture Strength and Young's Modulus of ZnO Nanowires. *Nanotechnology* **2007**, *18*, No. 205503.
(57) Chen, C. Q.; Shi, Y.; Zhang, Y. S.; Zhu, J.; Yan, Y. J. Size Dependence of Young's Modulus in ZnO Nanowires. *Phys. Rev. Lett.* **2006**, *96*, No. 075505.
(58) Hrkac, V.; Kienle, L.; Kaps, S.; Lotnyk, A.; Mishra, Y. K.; Schurmann, U.; Duppel, V.; Lotsch, B. V.; Adelung, R. Superposition Twinning Supported by Texture in ZnO Nanospikes. *J. Appl. Crystallogr.* **2013**, *46*, 396−403.
(59) Lao, C. S.; Liu, J.; Gao, P.; Zhang, L.; Davidovic, D.; Tummala, R.; Wang, Z. L. ZnO Nanobelt/Nanowire Schottky Diodes Formed by Dielectrophoresis Alignment across Au Electrodes. *Nano Lett.* **2006**, *6*, 263−266.
(60) Cardoso, G. W. A.; Leal, G.; Sobrinho, S.; Fraga, M. A.; Massi, M. Evaluation of piezoresistivity properties of sputtered ZnO thin films. *Mater. Res.* **2014**, *17*, 588−592.
(61) Cheng, G.; Miao, C.; Qin, Q.; Li, J.; Xu, F.; Haftbaradaran, H.; Dickey, E. C.; Gao, H.; Zhu, Y. Large Anelasticity and Associated Energy Dissipation in Single-crystalline Nanowires. *Nat. Nanotechnol.* **2015**, *10*, 687−691.
(62) Xu, F.; Qin, Q.; Mishra, A.; Gu, Y.; Zhu, Y. Mechanical Properties of ZnO Nanowires under Different Loading Modes. *Nano Res.* **2010**, *3*, 271−280.
(63) Miller, R. E.; Shenoy, V. B. Size-dependent Elastic Properties of Nanosized Structural Elements. *Nanotechnology* **2000**, *11*, 139.
(64) Cao, B.; Cai, W.; Zeng, H.; Duan, G. Morphology Evolution and Photoluminescence Properties of ZnO Films Electrochemically Deposited on Conductive Glass Substrates. *J. Appl. Phys.* **2006**, *99*, No. 073516.
(65) Zeng, H.; Cai, W.; Liu, P.; Xu, X.; Zhou, H.; Klingshirn, C.; Kalt, H. ZnO-Based Hollow Nanoparticles by Selective Etching: Elimination and Reconstruction of Metal−Semiconductor Interface, Improvement of Blue Emission and Photocatalysis. *ACS Nano* **2008**, *2*, 1661−1670.
(66) Zeng, H.; Duan, G.; Li, Y.; Yang, S.; Xu, X.; Cai, W. Blue Luminescence of ZnO Nanoparticles Based on Non-Equilibrium Processes: Defect Origins and Emission Controls. *Adv. Funct. Mater.* **2010**, *20*, 561−572.
(67) Janotti, A.; Van de Walle, C. G. Fundamentals of zinc oxide as a semiconductor. *Rep. Prog. Phys.* **2009**, *72*, No. 126501.
(68) Wei, B.; Zheng, K.; Ji, Y.; Zhang, Y.; Zhang, Z.; Han, X. Size-dependent Bandgap Modulation of ZnO Nanowires by Tensile Strain. *Nano Lett.* **2012**, *12*, 4595−4599.
(69) Han, X.; Kou, L.; Zhang, Z.; Zhang, Z.; Zhu, X.; Xu, J.; Liao, Z.; Guo, W.; Yu, D. Strain-Gradient Effect on Energy Bands in Bent ZnO Microwires. *Adv. Mater.* **2012**, *24*, 4707−4711.
(70) Faraji, N.; Ulrich, C.; Wolff, N.; Kienle, L.; Adelung, R.; Mishra, Y. K.; Seidel, J. Visible-Light Driven Nanoscale Photoconductivity of Grain Boundaries in Self-Supported ZnO Nano- and Microstructured Platelets. *Adv. Electron. Mater.* **2016**, *2*, No. 1600138.

DOI: 10.1021/acsomega.7b00041
ACS Omega 2017, 2, 2985−2993